# Performance and Control of a 30-cm-diam, Low-Impulse, Kaufman Thruster

ROBERT T. BECHTEL*
*NASA Lewis Research Center, Cleveland, Ohio*

**An experimental investigation was conducted to develop a 30-cm-diam, mercury bombardment thruster for potential space applications. Thruster operating efficiencies were improved by variation of the discharge-chamber geometry and magnetic field shape. A single, glass-coated system was used to achieve efficient thruster operation at lower specific impulse than previous bombardment thrusters. Propellant utilization efficiencies greater than 90% and discharge losses less than 200 ev/ion were attained. Estimated over-all thruster efficiency was about 58% at a specific impulse of 2200 sec. The investigation included a control system that afforded enough flexibility to throttle the ion beam current over a range of 2 to 1. This was accomplished without compromising expected lifetime of thruster components.**

## Nomenclature

| | | |
|---|---|---|
| $A_o$ | = | annular open area between distribution pole piece and baffle, cm$^2$ |
| $d$ | = | diameter, cm |
| $I_{sp}$ | = | specific impulse, sec |
| $J$ | = | neutral propellant flow, equivalent amp |
| $L/D$ | = | thruster-length/anode-diameter ratio |
| $l$ | = | length, cm |
| $\Delta V$ | = | potential voltage, v |
| $\eta$ | = | efficiency |
| $\epsilon$ | = | energy loss per beam ion, ev/ion |

***Subscripts***

| | | |
|---|---|---|
| $B$ | = | baffle |
| $I$ | = | discharge chamber |
| $OK,OM,OT$ | = | cathode, main, and total (flow), respectively |
| $P$ | = | distributor pole piece |
| $p$ | = | power (efficiency) |
| SC | = | screen collar |
| $T$ | = | total |
| $U$ | = | propellant utilization |

## Introduction

SPECIFIC impulses of 1500 to 3000 sec and thruster powers of 1200 to 3000 w are of interest for possible future solar electric applications.[1] Power matching is an important consideration for missions where solar-cell-array power sources have wide variations in output power. Throttling of the thruster is essential for such missions and imposes severe requirements on the thruster control system. Investigation of a prospective thruster for such applications at NASA Lewis Research Center, initially used a 30-cm-diam, mercury bombardment, Kaufman thruster which was scaled from the 15-cm-diam SERT II thruster. A number of changes in the discharge chamber geometry and ion extraction system were made to improve the thruster performance at low $I_{sp}$. Throttling capability was provided by a two-loop control system with a two-vaporizer propellant feed system, in contrast to the single vaporizer system used for the SERT II system.

Presented as Paper 69-238 at the AIAA 7th Electric Propulsion Conference, Williamsburg, Va., March 3–5, 1969; submitted March 19, 1969; revision received August 28, 1969.

* Aerospace Research Engineer.

## Thruster

The thruster (Fig. 1) employs a hollow cathode of the type used in the SERT II thruster.[2–4] The magnetic field required for efficient thruster operation is created by spacing permanent bar magnets around the circumference of the thruster body; it was shaped by mild steel pole pieces. The Alnico V magnets have a residual magnetism of 1.1 tesla and a coercive force of 500 oersteds. The dimensions shown in Fig. 1 were determined by the experimental program described herein.

Two types of ion extraction systems were used. One was a conventional two-grid, match-drilled system similar to that of SERT II[5]; the other was a single glass-coated grid.[6] The molybdenum two-grid system contained 2154 holes within a 28-cm diam. The holes in the 0.15-cm-thick screen electrode (positive high voltage) were 0.51 cm in diameter; those in the 0.21-cm-thick electrode (negative high voltage) were 0.40 cm in diameter. The holes were match-drilled in the two electrodes in a hexagonal array with a hole center-to-center spacing of 0.57 cm. This configuration provided an extraction open area of 74.7% comparable to the SERT II design.

The single, glass-coated grid was fabricated from commercially available, prepunched, 0.006-cm-thick molybdenum sheet. Glass coatings were fused to the molybdenum in several layers until the nominal glass thickness was 0.056 cm (Ref. 6). The open areas before and after coating were 50 and 40%, respectively.

Mercury propellant was supplied to the discharge chamber distributor and the hollow cathode by means of two electrically heated porous tungsten vaporizers.[4,5] With sufficient care to avoid entrapment of air in the mercury feed lines, adequate head pressure to maintain the liquid-vapor interface

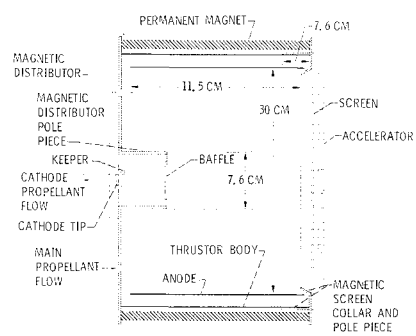


**Fig. 1 Sectional view of a 30-cm thruster.**

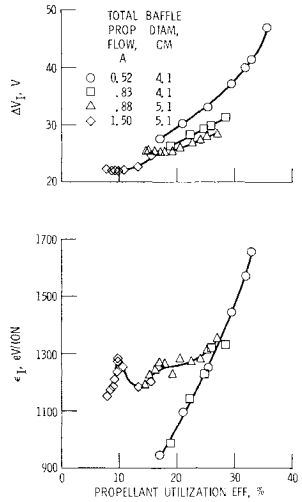


**Fig. 2 Performance of a 30-cm-diam thruster scaled from a SERT II thruster. $V_I$ = 2000 v; $V_T$ = 3300 v.**

at the porous tungsten plug, and sufficient time for thermal expansion effects to reach equilibrium, the neutral propellant flow rates were determined to better than 0.01 amp neutral flow, or 2% accuracy.

All ion thruster tests were conducted in a 1.5-m-diam, 4.5-m-long vacuum tank. The thruster was mounted in a metal bell jar separated from the tank by a 0.9-m-diam gate value. The tank was pumped by four 0.8-m-diam oil diffusion pumps with liquid-nitrogen-cooled baffles. Tank pressures were less than $1.2 \times 10^{-5}$ torr and bell jar pressure less than $3.0 \times 10^{-5}$ torr during thruster operation.

## Direct Scaling Effects and $L/D$

Initially, the thruster was scaled directly from an experimental SERT II, 15-cm-diam thruster.[3] All dimensions of the discharge chamber were doubled with the exception of the screen pole piece, which was unchanged. The previously described two-grid system was used. The number of magnets was unchanged, so as to provide approximately half the field strength and the same ratio of cyclotron radius to anode radius.[7] Figure 2 shows that the performance of the scaled-up 30-cm thruster fell far short of the SERT II performance of 85% propellant utilization efficiency at 250 ev/ion.[2] It was concluded that an ion bombardment thruster with a hollow cathode does not scale according to conventional scaling laws, probably because of the dependence of the discharge chamber voltage on the configuration. (In contrast, for a thruster with a thermionic emitter, the emission current is determined by the cathode temperature and the discharge voltage is determined by the voltage impressed by the discharge power supply,[7] so that independent control of the voltage and current can be realized.) The scaled hollow cathode thruster operates at unusually low discharge voltage (Fig. 2). Such thruster operation is characteristically accompanied by poor thruster performance.[3]

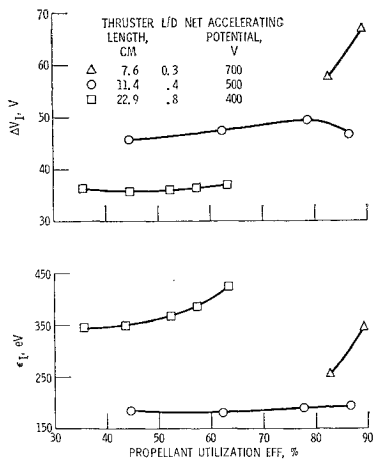


**Fig. 3 Effect of discharge chamber $L/D$ on thruster performance with single, glass-coated grid.**

Operation at $\Delta V_I > 32$ v was possible only by reducing the total propellant flow to far less than a scaled value. Although the performance at reduced propellant flows was the best for this thruster configuration, it still falls well below the 15-cm thruster performance in both propellant utilization efficiency $\eta_U$ and discharge losses $\epsilon_I$. Tests using a glass-coated grid provided similar results.

Higher $\Delta V_I$ and improved thruster performance were realized by increasing the magnetic field strength. This type of improvement was consistent with previous 15-cm thruster results.[3,5] Thus, with the exception of the initial scaled thruster, all 30-cm configurations employed 16 rather than 8 permanent magnets.

Further improvements in thruster performance were realized by reducing the thruster-length/anode-diameter ratio, $L/D$ from 0.8 (the value for SERT II) to 0.4; $\Delta V_I$ increased (Fig. 3a), $\epsilon_I$ decreased, and $\eta_U$ increased (Fig. 3b). However, the high $\Delta V_I$ (46–50 v) may compromise cathode lifetimes. Tests involving shorter thrusters with an $L/D$ of 0.3 were also conducted, but $\Delta V_I$ exceeded 60 v, and thruster operation became unstable. Thus, a configuration having an $L/D$ of 0.4 appeared best.

## Ion Extraction System

Both grid types were tested on thrusters with $L/D$'s of 0.8 and 0.4; however, the two grid types could not be operated at the same net accelerating potential $V_I$. The two-grid system required a minimum of 2500 v total, or $V_I$ 1500 v, to provide a beam current $J_B$ greater than 1.0 amp. Obtaining the same beam at lower voltage would require closer grid spacing. However, the center-support mounting system for the two-grid system would not maintain grid spacings of less than 0.20 cm during thruster operation. The maximum total voltage of the glass-coated grid was 1400 v, and $V_I$ was 700 v. Because the glass thickness was approximately 0.05-cm, the effective accelerating distance is less for a glass-coated grid than for a two-grid system. The reduced distance compensates in part for the reduced voltage, and $J_B > 1.0$ amp is possible with this system.

Figure 4 shows comparative performance for the various $L/D$ and grid-type combinations. The glass-coated grid provided lower $\epsilon_I$ for both $L/D$'s. The glass-coated grid

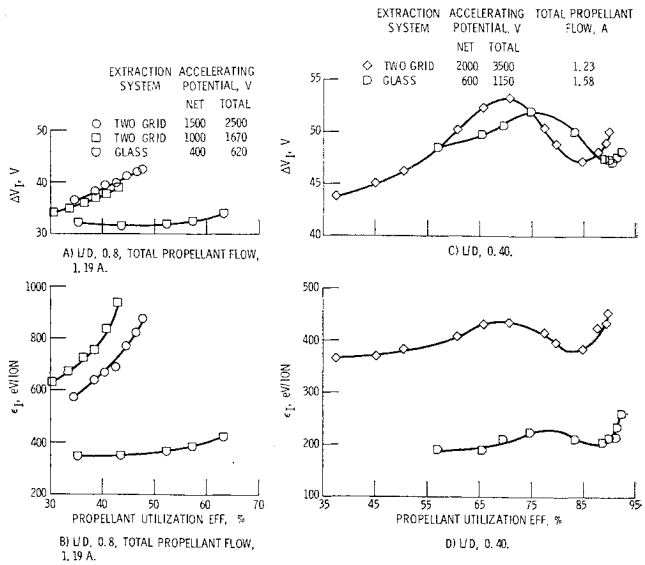


**Fig. 4 Comparison of glass-coated grid and two-grid extraction system. $L/D$ = 0.8; total propellant flow, 1.19 amp.**

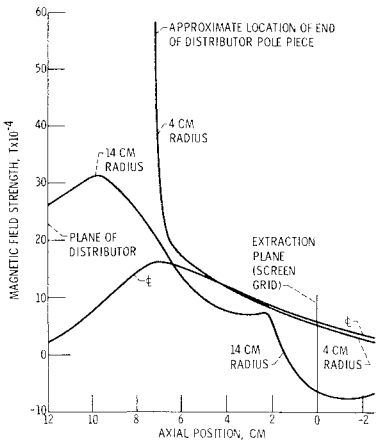


**Fig. 5 Axial component of magnetic field strength measured in thruster of Fig. 1 at three radial locations: centerline, 4 cm, and 14 cm.**

significantly improved the maximum obtainable $\eta_U$, although the shortening of the thruster alone was sufficient to increase $\eta_U$ to almost 90%, as shown in Fig. 3. A major difference in performance of the two $L/D$ configurations is the pronounced hump in the characteristic thruster performance curve of $\epsilon_I$ vs $\eta_U$ for the $L/D = 0.4$ cases (Fig. 4d). This hump could possibly cause difficulty in control of the thruster, but no difficulty was encountered in this program.

## Magnetic Field

The field was supplied by sixteen 0.63-cm-diam magnets. The magnetic field shape was determined primarily by the distributor pole piece length and diameter, the screen collar length, and the screen pole piece shape (Fig. 1). Previous testing[5] has indicated that the exact shape of the screen pole piece is not critical, although this component cannot be eliminated completely. The screen collar serves as an alternate magnetic path that permits lines of flux to intersect the anode rather than being shunted around the anode by the screen pole piece. The distributor pole piece serves to reduce the magnetic field to near zero in the region of the cathode and to provide high magnetic fields in the vicinity of the baffle. All baffles were solid disks located in the end plane of the distributor pole piece. Curves of the final magnetic field strengths at various locations in the thruster are shown in Fig. 5.

The effect of the length $l$ of the distributor pole piece on the characteristic curve of thruster performance is shown in Fig. 6. All data were taken at a constant cathode flow. The main propellant flow was adjusted to provide a $J_B$ of 1.5 amp. The $\Delta V_I$ for all data of Fig. 6 was in excess of 44 v. SERT II lifetests[2,3] indicated that operation at $V_I > 40$ v may not sufficiently guarantee cathode lifetimes. Thus, several configurations represented in Fig. 6 may be inadequate for a space-qualified thruster. Of the pole pieces tested, the 5.1-cm-long pole piece provides the best over-all performance. The performance curves for the shorter pole pieces are relatively flat and show less of an improvement in $\epsilon_I$ as $\eta_U$ is decreased. The performance curves for the longer pole pieces are similar in shape to the curve for $l = 5.1$ cm. The discharge losses decrease markedly with propellant utilization. Also, for these longer pole pieces and for a given $\epsilon_I$, $\eta_U$ decreases as $l$ increases.

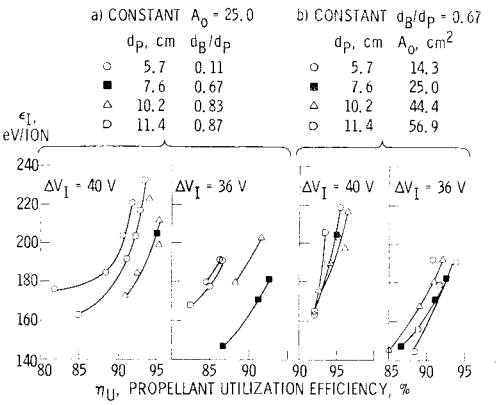


**Fig. 7 Effect of $d_P$ on thruster performance. Constant $d_B/d_P$ and $A_o$; $l_P = 5.1$ cm; $l_{SC} = 7.6$ cm; $J_B = 1.5$ amp; $V_I = 600$ to 625 v; single, glass-coated grid.**

Several pole piece diameters $d_P$ were also tested. The baffle variations were made concurrently to provide either a constant ratio of baffle diameter to pole piece diameter, $d_B/d_P$, or a constant annular open area $A_o$. Figure 7 shows the effects of these two variations on thruster performance. These data were obtained after screen collar modifications (described later) had effectively lowered $\Delta V_I$ to 40 v or less. Each of the characteristic curves were obtained by varying both cathode and main propellant flows to yield constant $\Delta V_I$ and $J_B$. This was done at various values of cathode emission current. The slopes of these curves are relatively unaffected by variations of $d_B$ and $d_P$, but there are shifts in magnitude of $\eta_U$ at a given $\epsilon_I$'s. Figure 8 (a cross-plot of Fig. 7 at $\epsilon_I = 180$ ev/ion) shows that a maximum $\eta_U$ occurs in the region of $d_B/d_P = 0.6$ to 0.7 for each $\Delta V_I$ (Fig. 8a). A voltage increase from 36 to 40 v increases $\eta_U$ at ratios other than optimum. The variation in $A_o$ has a smaller effect (Fig. 8b); except for one data point, $\eta_U$ is constant to within $\pm 1\%$ for either $\Delta V_I$.

The effect of varying the screen collar length $l_{SC}$ from 1.9 to 7.6 cm is shown in Fig. 9. The primary advantage in an $l_{SC}$ increase is the associated decrease in $\Delta V_I$ (Fig. 9a); the general level of $\epsilon_I$ remains unchanged (Fig. 9b), and $\eta_U$ is reduced by only 5–6%.

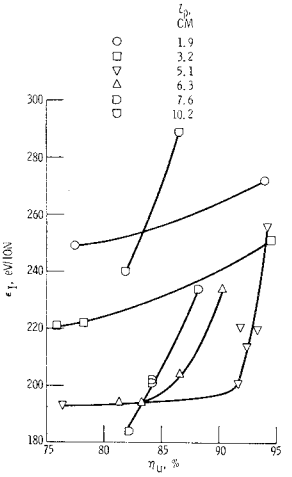


**Fig. 6 Effect of $l_o$ on thruster performance; $d_P = 7.6$ cm, $l_{SC} = 1.9$ cm, $d_B = 5.1$ cm; $J_B = 1.5$ amp, $V_I = 500$ to 600 v; $\Delta V_I = 44$ to 50 v; single, glass-coated grid.**

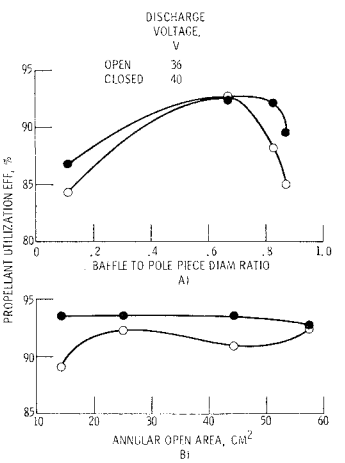


**Fig. 8 Effect of $d_P$ and $d_B$ on propellant utilization efficiency at constant discharge losses of 180 ev/ion (from data of Fig. 7).**

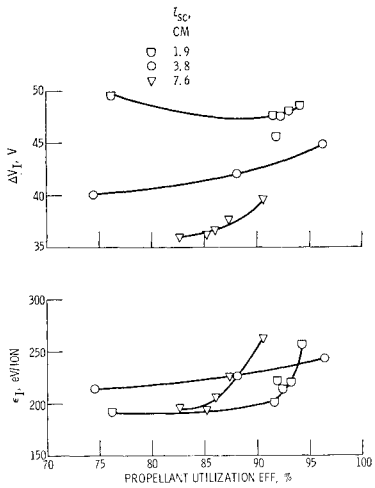


**Fig. 9 Effect of $l_{SC}$ on thruster performance. $d_P$ = 7.6 cm; $l_P$ = 5.1 cm; $d_B$ = 5.1 cm; $J_B$ = 1.5 amp; $V_I$ = 600 v; single, glass-coated grid.**

## Control Logic

The control system used for the 30-cm-diam thruster replaces the flow splitting orifice of the SERT II thruster[2,4] with a second vaporizer system and its servo loop (Fig. 10b), which controls the cathode propellant flow. The added servo loop senses $\Delta V_I$ and controls the propellant flow through the cathode vaporizer. The beam current-main propellant flow control loop remains unchanged. The discharge current is regulated at the preset value. The two control loops do interact, but by proper selection of the feedback time constants in the servo loop, undamped oscillations can be eliminated. The two-loop control logic has been successfully used to endurance-test a 15-cm-diam thruster for more than 1000 hr.

Thruster performance with the two-loop control system is shown in Fig. 11. The emission current was regulated at 8.5 amp. The main vaporizer servo loop controlled a 1.5-amp beam current. Figure 11a shows the effect of a variation of the $\Delta V_I$ set point; as it is increased, the cathode propellant flow is reduced. At the lower cathode flows the rate of change of $\Delta V_I$ decreases until unstable discharge operation results at cathode flows less than 67 ma. Because both beam current $J_B$ and emission current $J_I$ are constant, the voltage increase causes an increase in $\epsilon_I$ (Fig. 11b). As the cathode propellant flow is decreased, the main propellant flow also decreases until a minimum is attained at a cathode flow of 100 ma. As the cathode flow is further decreased and unstable operation is approached, the main propellant flow increases (Fig. 11c), the total propellant flow, however, remains nearly constant. Thus, $\eta_U$ increases until it reaches a maximum just before the onset of unstable operation (Fig. 11d).

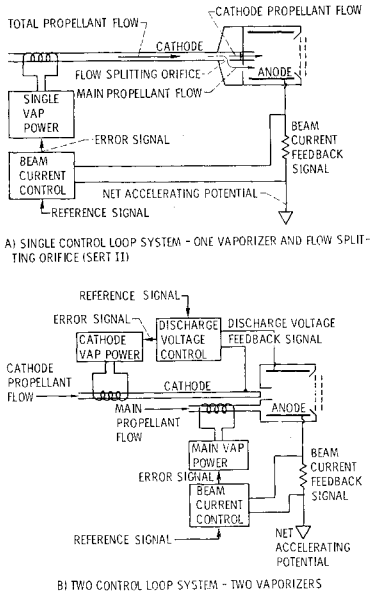


**Fig. 10 Schematic of two control logic schemes for ion bombardment thrusters.**

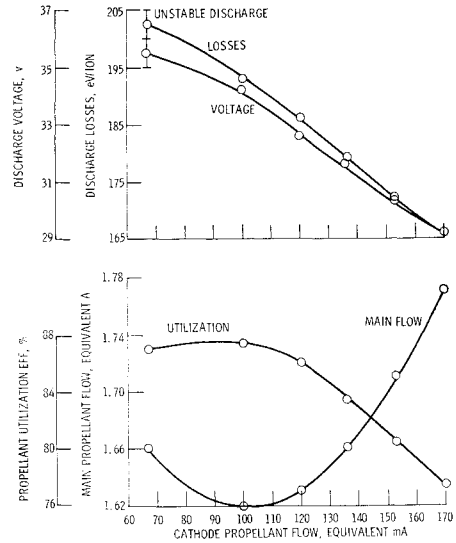


**Fig. 11 Thruster performance as a function of cathode propellant flow for various discharge voltage set points. $J_B$ = 1.5 amp; $J_I$ = 8.5 amp; $V_I$ = 600 v. Thruster of Fig. 1 with $d_B$ = 5.1 cm; single, glass-coated grid.**

## Throttling

Thruster operation over a range of $J_B$ was investigated with the two-loop system. The beam current was throttled to 45% of its typical 1.5-amp operating point by two methods (Fig. 12). The first was throttling at constant $\epsilon_I$ (by controlling for constant $\Delta V_I$). The emission-current/beam-current ratio and $V_I$ were maintained constant during the beam reduction. Since $\epsilon_I$ does not increase at the lower $J_B$, $\eta_U$ is lower. The total change was 16 percentage points for this throttling mode. The second method was throttling at constant discharge power (Fig. 12), holding $\Delta V_I$, $J_I$, and $V_I$ constant as $J_B$ was reduced. Thus, $\epsilon_I$ increased in inverse proportion to $J_B$. The total propellant flow did not decrease in proportion to $J_B$, and $\eta_U$ decreased about 9 percentage points. Although thruster operation was continuous between the two beam-current set points, thruster performance was not continuously documented in this mode.

In order to compare total efficiency ($\eta_T$) penalties for the two methods, the fixed power losses were estimated, based on existing 30-cm thruster data and SERT II data.[2] The combination of heater, neutralizer, and power losses is ap-

**Table 1 Summary of 30-cm-diam thruster performance**

| | |
|---|---|
| Thruster powers, w | |
| Beam (at 600 v) | 900 |
| Discharge (at 35 v) | 262 |
| Accelerator | 84 |
| Vaporizer/feed[a] | 13 |
| Cathode tip/keeper[a] | 13 |
| Neutralizer[a] | 55 |
| Thruster efficiencies, % | |
| Power | 68 |
| Propellant utilization, excluding neutralizer | 89 |
| Propellant utilization, including neutralizer estimate[b] | 86.3 |
| Total, excluding neutralizer | 60.4 |
| Total, including neutralizer estimate | 58.3 |

[a] Estimate based on current SERT II data.
[b] Propellant flow of 0.05 amp added to total thruster flow to allow for operation of a plasma bridge neutralizer.[3]

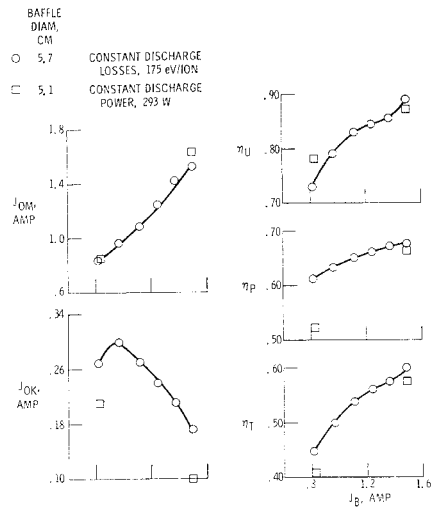


**Fig. 12 Two methods of beam current throttling of thruster with glass-coated grid ($V_I$ = 600 v; $\Delta V_I$ = 34.3 and 35 v) and comparison of thruster efficiencies.**

proximately 165 w (Table 1). A single, over-all performance value based on these estimates is also given in Table 1. The results (Fig. 12) show that in throttling at constant discharge power, the reduced beam power results in a power efficiency ($\eta_P$) penalty. However, in throttling at constant $\epsilon_I$, some of the beam power loss is offset by the imposed decrease in discharge power. As noted before, the penalty to $\eta_U$ is less for the constant-power mode than for the constant-$\epsilon_I$ mode. Inasmuch as $\eta_T = \eta_P\eta_U$, the gain in $\eta_U$ tends to offset the loss in $\eta_P$. For a 2:1 reduction in beam current, the decrease in $\eta_T$ is ~15 percentage points (or ~25% of $\eta_T$) for either mode. Thus, continuous throttling of the two-control-loop system and 30-cm thruster is possible. The $\eta_T$ penalty of ~25% is primarily in either $\eta_P$ or $\eta_U$, depending on the throttling mode used.

## Conclusions

This investigation has determined the design of a 30-cm-diam Kaufman thruster with a specific impulse ($I_{sp}$) range of 1500 to 3000 sec, and thruster power range of 1200 to 3000 w. Included is a control logic system that permits throttling of the thruster from rated beam current to 45% output without compromising expected lifetimes.

Results of tests of a scaled-up version of the 15-cm-diam SERT II thruster showed that a thruster using a hollow cathode does not scale directly. The probable reason is the dependence of the discharge voltage on discharge chamber geometry.

Improved performance was realized at $I_{sp} < 3000$ sec by the use of a single, glass-coated grid extraction system. This system was directly responsible for improved thruster performance at net accelerating potentials of less than 1000 v.

Thruster performance was improved by reducing the thruster $L/D$ from the SERT II value of 0.8 to 0.4. This shorter $L/D$, combined with the best magnetic field shape realized from pole piece variations, led to thruster performance in excess of 90% propellant utilization and less than 200 ev/ion discharge losses. Total thruster efficiency was 57 to 60% at an $I_{sp}$ of 2200 sec.

The control logic uses a two-loop, two-vaporizer system as opposed to present, SERT II single-vaporizer systems. This system provided sufficient flexibility to throttle the beam current to 45% of its original value of 1.5 amp. This was accomplished without increasing discharge current and voltage which, in turn, could compromise expected lifetimes. Preliminary throttling was carried out either by maintaining constant discharge power or constant discharge losses, with a resulting total efficiency decrease approximately 16 percentage points in either case.

## References

[1] Mullin, J. P., Barber, T., and Zola, C., "Solar-Cell-Powered, Electric Propulsion for Automated Space Missions," AIAA Paper 68-1120, New York, 1968; also *Journal of Spacecraft and Rockets*, Vol. 6, No. 11, Nov. 1969, pp. 1217–1226.

[2] Byers, D. C. and Staggs, J. F., "SERT II Flight-Type Thruster System Performance," AIAA Paper 69-235, Williamsburg, Va.; also "SERT II: Thruster System Ground Testing," *Journal of Spacecraft and Rockets*, Vol. 7, No. 1, Jan. 1970, pp. 7–14.

[3] Bechtel, R. T., Csiky, G. A., and Byers, D. C., "Performance of a 15-Centimeter Diameter, Hollow-Cathode Kaufman Thruster," AIAA Paper 68-88, New York, 1968.

[4] Kerslake, W. R., Byers, D. C., and Staggs, J. F., "SERT II Experimental Thruster System," AIAA Paper 67-700, Colorado Springs, Colo., 1967; also "SERT II: Mission and Experiments," *Journal of Spacecraft and Rockets*, Vol. 7, No. 1, Jan. 1970, pp. 4–6.

[5] Bechtel, R. T., "Discharge Chamber Optimization of the SERT II Thruster," AIAA Paper 67-668, Colorado Springs, Colo., 1967.

[6] Banks, B., "Composite Ion Accelerator Grids," Electrochemical Society Third International Conference on Electron and Ion Beam Science and Technology, Boston, Mass., May 1968.

[7] Reader, P. D., "Experimental Effects of Scaling on Performance of Ion Rockets Employing Electron-Bombardment Ion Sources," Paper 1781-61, 1961, ARS.

[8] Rawlin, V. K. and Pawlik, E. V., "A Mercury Plasma-Bridge Neutralizer," AIAA Paper 67-670, Colorado Springs, Colo., 1967.